Point-of-Care Devices to Detect Zika and Other Emerging Viruses

Point-of-Care Devices to Detect Zika and Other Emerging Viruses

Helena de Puig[1,2], Irene Bosch[3], James J. Collins[1,2,4,5], and Lee Gehrke[1,6]

[1]Institute for Medical Engineering and Science, Massachusetts Institute of Technology, Cambridge MA; [2]Wyss Institute, Boston MA; [3]E25Bio, The Engine, Cambridge MA; [4]Department of Biological Engineering, Massachusetts Institute of Technology, Cambridge MA; [5]Broad Institute of MIT and Harvard; [6]Department of Microbiology, Harvard Medical School, Boston MA

Lee Gehrke: lgehrke@mit.edu ORCID: https://orcid.org/0000-0002-9387-8212
Helena de Puig: hpuig@mit.edu ORCID: https://orcid.org/0000-0002-5368-6996
Irene Bosch: ibosch@e25bio.com ORCID: : https://orcid.org/0000-0003-1352-5888
James J. Collins jmjc@mit.edu ORCID: https://orcid.org/0000-0002-5560-8246

Corresponding author: Lee Gehrke: lgehrke@mit.edu

Shortened running title: Rapid diagnostics for Emerging Viruses

Keywords: rapid diagnostic, virus, synthetic biology, lateral flow immunoassay, monoclonal antibody, synthetic genetic circuit

Abstract:

Rapid diagnostics are critical components of informed patient care (point of care devices) and public health monitoring (surveillance applications). We propose in this Review that, among the many rapid diagnostics platforms that have been tested or are in development, lateral flow immunoassays (LFIA) and synthetic biology-based diagnostics represent the best overall options for ease of use, scalability for manufacturing, sensitivity and specificity performance. This Review discusses the identification of LFIA monoclonal antibody pairs that detect and distinguish closely related pathogens in combination with functionalized multicolored nanoparticles and computational methods to deconvolute data. We also discuss the promise of synthetic biology-based diagnostics, based on synthetic genetic circuits, that detect even single nucleotide changes. LFIA and synthetic biology are perhaps bookend membrane diagnostic methods in terms of history of the spectrum of technologies, and their combined or parallel uses may represent the future of scalable rapid diagnostics.

Introduction

Human health monitoring, as well as disease prevention and treatment, are informed to great benefit by accurate and timely detection and identification of pathogens. This is the domain of rapid diagnostics, which detect low concentrations of ligands to reveal pregnancy, detect viral and bacterial pathogens, and track markers that reflect human physiology. As the name implies, a rapid diagnostic test is designed to report data quickly; that is, in under approximately twenty minutes. It can be used as a point-of-care instrument, meant to inform immediate patient care at the bedside, or as a surveillance device for epidemiology, as applied to routine monitoring for the appearance or number of pathogens. In some examples, the basic design of rapid tests has remained relatively unchanged over decades; this is true for paperfluidic lateral flow devices. In other cases, a new era of rapid diagnostics is emerging in the form of synthetic biology (synbio) tests that can be activated by re-hydration from a stable desiccated form to turn on genetic switches and specific amplification reactions that can detect single nucleotide sequence variations.

In the first section of this review, we describe recent single and multiplexed paperfluidic lateral flow immunoassay (LFIA) devices to detect closely related viruses, focusing on combinatorial monoclonal antibody pairs that discriminate very closely related proteins. Included in this section is a description of computational methods that evaluate detection thresholds and calculate area-under-the-curve (AUC) to assign performance values. LFIA technologies were reviewed recently by Banerjee and Jaiswal(1). Wild(2) has edited an excellent handbook that emphasizes immunoassays, but also describes

terminology and definitions that are relevant to describing the development and performance of rapid diagnostic devices. In the second section of this review, we discuss recent advances in synthetic biology approaches for developing rapid diagnostic devices. Unlike LFIA, which was introduced in the 1980's(3), synthetic biology was introduced near twenty years ago(4-7). Recent papers summarize contributions of synthetic biology to diagnostics development(8-10). This Review focuses on the successes and challenges of developing and distributing synthetic biology devices for broad use. Lateral flow and synbio approaches are distinct, but their complementary features may be the future of rapid diagnostics for detecting pathogens that threaten human health.

Lateral Flow Immunoassays for Detecting and Distinguishing Closely-Related Viruses

Many human tropical viral infections present with similar symptoms; that is, fever, rash, headache, and malaise. In the absence of diagnostic tests, it is often very difficult to distinguish among dengue fever, Zika disease, and Chikungunya disease. Most infections are diagnosed as "fevers of unknown origin" because facilities, resources, or diagnostic devices are not available to detect and distinguish the pathogen(10). This problem is exacerbated by virus families that have distinct but related species (*e.g.* dengue viruses and Zika virus) that cause distinct pathologies despite their homologous viral proteins.

Our recent work has included a focus on developing and testing rapid diagnostics to detect and distinguish the four dengue virus serotypes, as well as Zika virus(11). This

was a challenging problem because the four dengue serotype NS1 proteins share about 80% homology, meaning that antigenic determinants will be shared, complicating strategies to distinguish them in LFIA. Dengue and Zika NS1 proteins have greater than 50% homology, and though this is less similarity than among the dengue serotypes, crossover interference in dengue-Zika diagnostics is a significant problem(11). To initiate the process of developing LFIA to detect and distinguish the four dengue serotypes, as well as Zika virus, we immunized mice with each of the non-structural-1 (NS1) proteins. The initial identification of antibodies for use in diagnostics is tedious and is most often accomplished by ELISA in 96- or 384-well plates. However, the behavior of a monoclonal antibody in ELISA is not necessarily predictive of its behavior in LFIA; therefore, device developers recommend testing the selected antibodies in the lateral flow immunoassay format at the earliest opportunity in the development pipeline(2).

A matrix approach (Figure 1) is used to test the binding characteristics of paired monoclonal antibodies in ELISA. The antibodies indicated by clone numbers on the Y axis were, immobilized on the LFIA membrane, while the antibodies on the X axis were conjugated to gold nanoparticles. Also shown on the X-axis, for each antibody, are the dengue 1-4 NS1 antigens, or the Zika virus (ZV) NS1 protein antigens used with the dipstick. Every combination was tested, and the darkest green is the strongest binding signal, and white color signifies no color (no detectable binding at the LFIA test line. The data demonstrate differential binding properties among the monoclonal antibody pairs. For example, mAb 243 showed preferential binding for dengue serotype 2 NS1 in

combination with mAbs 323, 136, 243, 29, and 1, but little binding to Zika virus NS1. Conversely, antibody 136 bound poorly to dengue serotype 4 NS1, but bound to other dengue serotype NS1 and Zika virus NS1 in pairing with other monoclonal antibodies. mAb 912 showed specificity for dengue serotype 1, while mAbs 29 and 900 cross-reacted among several dengue serotype NS1 proteins. These data demonstrated that, although the NS1 proteins of the dengue serotype 1-4 and Zika viruses are homologous and elicit many cross-reactive antibodies, it was possible to identify antibody pairs that distinguished the individual pathogens. These antibody pairs were used in LFIA to test patient serum samples, and the resulting data, evaluated by through receiver-operator curve (ROC) analysis, demonstrated excellent device performance(11).

In gold nanoparticle-based LFIA, a positive test signal is observed and detected as a red-purple band or dot that forms as the visible accumulation of gold nanoparticles. Gold nanoparticles are available in commercial kits for rapid and simple antibody conjugation; however, the cost is generally prohibitive for manufacturing scale-up. Alternatively, laboratory and commercial nanoparticle syntheses are relatively simple, can be performed with both gold and silver salts, and can yield a rainbow of different-colored nanoparticles(12-15). A consistent goal of LFIA is to obtain the greatest amount of information from the smallest patient sample size, in the shortest amount of time, and with the greatest sensitivity, sensitivity, and limit of detection. Multiplexing; that is, detecting multiple pathogens in a single test, is an obvious approach, but one that is often fraught with non-specific binding interactions and cross-reactivity. However, careful selection of antibody pairs--though time-consuming and tedious--can generate

rigorous multiplexed diagnostics. The results presented in Figure 2 show the detection of three viral antigens; that is, dengue virus NS1 protein, Chikungunya virus envelope proteins, and Zika virus NS1 protein in a multiplexed assay. These three viruses can co-circulate, and the acute symptoms of the infections are initially very similar. Moving from left to right in the figure, the antigens are first tested individually, showing that there is little cross-reactivity. Next, combinations of two sample antigens are tested (DZ: dengue and Zika virus NS1 proteins; ZC; Zika NS1 and Chikungunya envelope protein; DC: dengue NS1 and Chikungunya envelope), Little cross-reactivity is observed at the omitted antigen test area. Finally, all three antigens are combined (D/Z,C). The data demonstrate the functionality of a multiplexed test for dengue, Zika, and Chikungunya viruses using a single color gold nanoparticle. Although the single antigen tests (D,Z,C) show little cross reactivity at the other test areas, a potential disadvantage of this test is that it is difficult to determine if there is cross reactive binding if two positive signals appear, suggesting a co-infection. In the following section, we discuss the use of multicolored nanoparticles, which can be effective in evaluating cross reactivity in multiplexed tests.

The use of multi-colored nanoparticles is advantageous in LFIA because it facilitates test multiplexing with the concurrent evaluation of cross reactivity. Multicolored silver nanoparticles can be synthesized using a seed-mediated growth method(16). Colored nanoparticles allow the user to see not only the positive test signal, but also to assess cross reactivity. Yen *et al.(15)* demonstrated that Ebola, Yellow Fever, and Dengue virus antigens could be detected using colored silver nanoparticles, where the

three assays were multiplexed into a single dipstick test. The addition of color adds a second specificity parameter in the tests; that is, in addition to test signal position on the strip, color is also present. In control reactions, the identity of the immobilized antibody should match with the identity of the corresponding antibody conjugated to the colored nanoparticle. The absence of a match, indicated by unexpected color, suggests non-specific cross reactive binding. With strong signals, the colors are easily distinguished; however, with weaker signals or in the case of cross reactivity, the colors can be less discernible by eye.

Imaging and computational methods are used to quantify individual nanoparticle signals by RGB (red-green-blue) analysis in open source applications (ImageJ); further, principal component analysis (PCA) clusters the data for objective determination of test specificity (identifying true positive signals) and sensitivity (identifying true negative signals)(15) (Figure 3). At the completion of the dipstick run, the strips are dried and photographed, often using a mobile phone camera. The resulting image is imported into image analysis software, such as ImageJ for RGB separation. These results are then imported into a MatLab script that performs the principal component analysis. An important advantage of the image analysis and PCA is that the data are objective, quantified, and expressed in a statistically rigorous output. The results (Figure 3c) demonstrate that each pair's signal is clearly separated from other pairs; therefore, the detection is unequivocal. Cross reactive binding is not observed in Figure 3, but if it were present, clusters would be shifted or unexpected clusters would appear. A potential disadvantage of the image analysis and PCA is that post-run time is required

to take the images and process the data. The added time need not be significant, however, because the use of standardized test dipsticks permits development of automated scripts that run on mobile phones to take images and process the data, delivering a result/diagnosis. After standardizing a detection platform with multiplexing and colored nanoparticles, the analysis should add only a few minutes to time-to-result, as compared to single and one-color runs.

Synthetic biology-based diagnostic tests

The interactions that regulate antibody-antigen binding –such as in LFIA and ELISA- are complex, and involve hydrogen bonds, hydrophobic interactions, electrostatic and van der Waals forces(17). In contrast, nucleic acid recognition is straightforward and predictable. Base pairs of the four nucleic acid bases bind through Watson-crick pairing: adenine (A) binds to thymine (T) (or uracyl (U) in the case of RNA) through two hydrogen bonds and guanine (G) binds to cytosine (C) through three hydrogen bonds. Due to the simplicity of DNA binding, it is possible to predict the binding thermodynamics, secondary structure and hybridization of nucleic acid sequences in silico. Nucleic acid-based diagnostics capitalize on DNA or RNA base pair recognition.

The current gold standard of nucleic acid testing is polymerase chain reaction (PCR) (18; 19). PCR has high sensitivity and specificity, however, it is typically avoided in POC applications, as it is slow and requires a thermal cycler, fixed location, expensive materials and trained personnel(20; 21). PCR is susceptible to contamination, and PCR inhibitors are present in human blood and body fluids, thus careful sample preparation is essential (22). Moreover, PCR reagents (proteins and dyes) are sensitive to humidity, light and temperature and require cold chain transport.

Several DNA amplification techniques exist that alleviate the use of a thermal cycler(23). Low temperature isothermal amplification technologies have been developed and extensively studied and contrasted in literature reviews(20; 24-26). Isothermal amplification technologies include nucleic acid sequence-based amplification(27) (NASBA), helicase-dependent amplification (HDA), recombinase polymerase amplification (RPA), rolling circle amplification (RCA), and loop-mediated isothermal amplification (LAMP), among others. Frequent issues with isothermal amplification techniques involve off-target amplification, the difficulty to multiplex the assays, the need for a purification and fixed location, and the strict requirement of a cold-chain transport of reagents.

Cell-free synthetic biology-based diagnostics

New technologies based on synthetic biology allow for the detection of DNA and RNA sequences in a freeze-dried format that is stable for long-term storage at room temperature. Synthetic biology combines biological sciences with engineering principles to create new biomolecular functions for practical applications. In the context of POC diagnostics, synthetic biology efforts have been focused on building sensors (i.e. toehold switches) that are coupled to a measurable signal, such as the production of an output protein. These synthetic gene circuits arise from the engineered assembly of natural molecular components. During the last years, our lab has developed a platform for rapidly creating synthetic biology-based diagnostics that are inexpensive, portable, and easy to use(28; 29). The platform is a combination of two technologies: programmable molecular sensors called RNA toehold switches and an *in vitro* cell-free expression system freeze-dried onto paper discs. The toehold switch sensors can be rationally designed to bind and

sense virtually any RNA sequence(30). DNA encoding the sensors can be lyophilized onto paper along with cell-free transcription and translation components and these materials have been shown to remain stable at room temperature for over one year. The system is activated by the addition of a sample containing the target RNA(29). The freeze-dried, paper-based, cell-free system allows for the implementation of the toehold switch sensors in a sterile, abiotic manner that can be easily developed into a point-of-care diagnostic. Because these systems perform *in vitro*, they do not face the complexities poised by cell-based synthetic biology approaches of importing the biomolecular components into the intracellular space, making them easily modified and excellent platforms for bioengineering.

Toehold switch sensors combined with freeze-dried cell-free exoression systems have been used to design paper-based sensors to detect antibiotic resistance markers(28), Ebola virus(28), Zika virus(29) and to study the microbiome(31). After these proof-of-concept demonstrations, several challenges remain for the practical implementation of paper-based diagnostics, such as meeting the detection thresholds required for field use. To overcome this limitation, amplification strategies (i.e. PCR, NASBA or RPA) for incoming nucleic acids have been combined with toehold switch detection(29; 31), showing limits of detection within the range of interest for many clinical applications. The advantages of cell-free synthetic biology-based diagnostics over qPCR are their cost and the ability for multiplexed detection. RNA can be quantified in 3-5h at a cost of between $2-$16 per transcript(31) at a low temperature. Moreover, in addition to fluorescence outputs, the sensors can be designed to produce luminescence and also enzymes that

generate color changes visible to the naked eye(29), which is an interesting feature for POC applications in low-resource settings lacking technical infrastructure.

CRISPR Cas-based diagnostics

A newer class of diagnostic devices emerged with the discovery of CRISPR-Cas systems. CRISPR-based diagnostics leverage the programmable RNA-guided endonucleases (Cas enzymes) of CRISPR-associated microbial adaptive immune systems. Cas enzymes have evolved to recognize specific target foreign nucleic acid sequences and to subsequently neutralize them through cleavage. Cas enzymes are easily programmable to detect any nucleic acid sequence of interest by simply changing the sequence of the guide RNA. Due to their high specificity and enzymatic activity, CRISPR-Cas systems have rapidly led to the development of a new class of infectious disease diagnostics.

Cas9: CRISPR-Cas9 was the first protein of the CRISPR family used in diagnostic applications. CRISPR-Cas9 diagnostics typically use a Cas9 enzyme to cleave a nucleic acid sequence of interest and then use a different technology, such as toehold switches(29), sequencing(32), optical DNA maps(33), qPCR(34-37) or electrochemistry(38; 39) as a readout. Portable, freeze-dried diagnostics using CRISPR-Cas9 combine Cas9 with isothermal nucleic acid amplification (NASBA) and toehold switch sensors to accurately distinguish between closely related virus strains(29). Pardee et al. appended a synthetic trigger sequence to NASBA-amplified viral RNA and used a sgRNA-Cas9 complex to cleave the resulting dsDNA (Figure 5a). The presence or absence of a strain-specific PAM resulted in truncated or full-length DNA fragments upon Cas9 cleavage. Full-length strands, but not the truncated strands, activated the toehold trigger switch, which induced a color change on a paper disc, allowing reliable strain

differentiation. This approach enabled the detection of single nucleotide polymorphisms (SNP) (Figure 5b). In different applications, catalytically dead Cas9 enzymes (dCas9), which do not induce DNA cleavage, have also been used to capture specific DNA sequences followed by detection by electrochemistry(38; 39), or fluorescence in situ hybridization(40).

These DNA sensing technologies have great diagnostic potential. However, they are inherently limited by the one to one stoichiometry of Cas9. Consequently, recent focus has been recently placed on approaches using Cas enzymes that exhibit multi-turnover kinetics and are thus able to provide a signal amplification upon detection of the target nucleic acid sequence.

Cas12, Cas13: exploiting collateral cleavage: More recent applications of CRISPR for the development of infectious disease diagnostics take advantage of collateral cleavage induced by Cas12, Cas13 or Cas14 nucleases. The first of these platforms is termed specific high-sensitivity enzymatic reporter unlocking(SHERLOCK), and combines isothermal recombinase polymerase amplification (RPA) or reverse transcription (RT)-RPA with Cas13a cleavage(41). The gRNA-Cas13a complex activates after specific binding to the target RNA sequence. It then engages in collateral cleavage of nearby reporter RNA coupled to a quenched fluorescent reporter, providing a fluorescent signal for pathogen detection (Figure 6a). The high specificity of the technique allows to differentiate between closely related Zika virus strains and Dengue viruses (Figure 6b), and distinguish between K. pneumoniae isolates with different resistance genes(41), in a freeze-dried, stable format. Gootenberg et al. introduced SHERLOCKv2 with

improvements that include single reaction multiplexing with orthogonal CRISPR enzymes (Figure 6c), quantitative target detection, enhanced sensitivity, and portability(42). Detection of up to four targets is achieved by combining multiple Cas13 and Cas12 nucleases with nucleic acid-fluorescent reporter complexes that provide signal detection at different wavelengths. In addition, assays can be coupled to a paper-based lateral flow readout, increasing the portability of the assay for POC applications in low-resource settings (Figure 6d).

In a further advance, Myhrvold et al. combined SHERLOCK with heating unextracted diagnostic samples to obliterate nucleases (HUDSON)(43), which eliminates the need for nucleic acid extraction and allows pathogen detection directly from bodily fluids. In HUDSON, heat and chemical reduction inactivate the high levels of nucleases present in body fluids, followed by lysis of viral particles, which releases nucleic acids into solution. HUDSON combined with SHERLOCK allows highly sensitive detection of dengue virus in patient samples of whole blood, serum, and saliva within 2 h. The authors also demonstrate assay specificity and adaptability by distinguishing between four Dengue virus serotypes and developing an assay for detection of six common HIV reverse transcriptase mutations within 1 week.

A similar technique, termed DNA endonuclease-targeted CRISPR trans reporter (DETECTR), combines isothermal RPA with Cas12a(44) or Cas14a(45) enzymatic activities. In DETECTR, binding of the crRNA-Cas12a complex to target ssDNA or dsDNA induces indiscriminate cleavage of ssDNA that is coupled to a fluorescent reporter. DETECTR was used to distinguish between human papillomavirus 16 (HPV16) and

HPV18 in crude DNA extracts from cultured human cells and from clinical samples (44). Crude extracts from 25 human samples were tested using DETECTR, and the results agreed to those of an approved PCR-based assay. Overall, CRISPR-Cas based diagnostics combine the high specificity of CRISPR-Cas systems with isothermal amplification technologies to provide POC rapid diagnostic tests that can reach limits of detection comparable to qPCR, at a fraction of the cost, in a field-deployable format.

CRISPR-based diagnostics are hold great promise for POC applications due to their sensitivity, specificity, multiplexing capacity, ease of use, cost and their capacity to detect virtually any nucleic acid sequence. However, they are relatively new and have been untested beyond proof of concept applications, making it difficult to estimate their potential impact in the POC diagnostics field. CRISPR-based diagnostics can be compared with other nucleic acid detection methods, such as PCR. In contrast with PCR, SHERLOCK and DETECTR combine an isothermal amplification step with a detection step that further amplifies the signal and also provide increased specificity based on crRNA target recognition. In addition, CRISPR-based assays can be freeze-dried and easily deployed as they operate at low temperatures, without the requirement of a thermocycler. While some isothermal amplification technologies, such as RPA can also run under similar conditions, they often suffer from low specificity, due to low-temperature primer annealing. In contrast, CRISPR effectors have evolved to increase the specificity of recognition of nucleic acids at physiological temperatures, widening their applications in POC diagnostics.

Technical Challenges in developing POC diagnostics for outbreaks

Assessing diagnostic performance

Assessing diagnostic accuracy is important to evaluate the performance of POC diagnostic tests. In order to make a decision to promote the clinical use of a new assay, evidence is required that using the new test either increases accuracy over previous assays, or has equivalent accuracy but offers other advantages(46). Diagnostic accuracy refers to the ability of the diagnostic test to distinguish between the absence or presence of disease. Accuracy can be quantified by measures such as sensitivity, specificity, predictive values, likelihood ratios or Receiver Operating Characteristic (ROC) curves.

A perfect diagnostic should completely discriminate between infected and uninfected subjects. For binary tests that distinguish the presence or absence of disease, the cut-off parameter is used to divide the test results into categories, where values above the cut-off are scored positive for the presence of disease, and values below the below the cutoff indicate the absence of disease. However, a perfect diagnostic that can completely differentiate the population does not exist. Sometimes, subjects without disease can show results above the cut-off (false positives, FP) and subjects with disease can show values below the cut-off (false negatives, FN). Therefore, the cut-off divides the population into four subgroups:

- True positive (TP): patients with the disease with diagnostic results above the cut-off

- False positive (FP): patients without the disease with diagnostic results above the cut-off
- True negative (TN): patients without the disease with diagnostic results below the cut-off
- False negative (FN): patients with the disease with diagnostic results below the cut-off

To calculate the sensitivity, specificity and predictive values, a typical approach is to make a 2x2 table (Figure S1-A), according to a gold standard (reference method). Sensitivity relates to a diagnostic's potential to recognize subjects with the disease, and is defined as the probability of obtaining a positive test result in confirmed infected patients. Specificity is defined as the probability of obtaining a negative test result in confirmed uninfected patients, and expresses the diagnostic's potential to recognize patients without the disease. Positive predictive value (PPV) indicates the probability of having the disease in a subject with a positive test result, and negative predictive value (NPV) describes the probability of not having the disease in patients with a negative test result. Sensitivity and specificity are not influenced by the prevalence of the disease in the population. In contrast, PPV and NPV are influenced by the disease prevalence in the examined population. Therefore, NPV and PPV from one study cannot be transferred to settings with different disease prevalence in the population.

The ROC curve (Figure S1-B) shows how the values of sensitivity and specificity change with varying thresholds across all possible values. The graph plots sensitivity (true positive rate) against 1-specificity (false positive rate). The ROC curve goes from

the point where sensitivity and 1-specificity are both 1 (upper right corner) and the point where sensitivity and 1-specificity are both zero (lower left corner). The shape of a ROC curve and its area under the curve (AUC) can be used to estimate the discriminative power of a diagnostic. ROC curves that are closer to the upper left corner of the graph have a larger AUC and are better in discriminating between infected and non-infected patients. The AUC can have any value between 0 and 1. A perfect diagnostic test has a AUC of 1, while a nondiscriminating test has an area of 0.5.

The measures of diagnostic accuracy are standardized, and excellent resources on the topic can be found in both the Cochrane collaboration and The Standards for Reporting of Diagnostic Accuracy (STARD) databases. However, diagnostic accuracy measurements are extremely sensitive to the study design. For example, small sample sizes, differences in study populations or differences in study methods can lead to inaccurate results. Moreover, in POC applications, physical constraints such as limited water, temperature variations, unreliable power sources or reagent stability during storage or transportation can also have a large impact on the performance of a diagnostic.

Regional and population variations on diagnostic test performance

Many factors influence the performance of POC diagnostics, such as the prevalence of disease, the age of the patient, the acquisition of partial immunity and the coinfection with other diseases. Therefore, diagnostic tests need to be evaluated in a clinically-relevant population. The term commonly used to describe this heterogeneity is

spectrum bias, and occurs when diagnostic test performance varies across patient subgroups and a study of that test's performance does not adequately represent all subgroups. Sources of *spectrum bias* include differences in demographic features within the population, disease severity, disease prevalence, and distorted selection of participants in the analysis. Therefore, during the development of POC diagnostics it is important to validate the assays in the settings and the population in which they will be used.

Specimen collection

Sample collection and processing are critical steps in diagnosis. Nevertheless, the manually intensive activities of sample collection and processing are some of the most error-prone steps in diagnostics. Collecting a wrong sample type, for example, can reduce the accuracy of a diagnostic test(47). Sample collection technologies that are used in high resource settings might not be available in POC applications during outbreaks. Thus, POC assays would ideally be packaged and tested with a paired specimen collection device for each POC application to ensure lower variability of results.

Incorporating rapid diagnostics data into medical records and shared public health resources

Rapid diagnostics inform clinical care decisions and provide epidemiological data through surveillance assays. An important challenge for future work in the rapid diagnostic field is in defining how rapid diagnostic test data are incorporated into a

patient's permanent medical record, and how the global community will define standards for collecting, storing, accessing, and protecting patient data. Although the use of medical electronic records is expanding, virus diagnostic results are generally not part of the HL7 interoperable medical record. Today there are few examples for standardized rapid test reporting platforms for other infectious diseases like Malaria using District Health Information Systems (DHIS2) with accumulated success in multiple countries(48).

Summary Points

1. Lateral flow immunoassays (LFIA) and synbio diagnostics are widely separated on the technology spectrum but offer complementary approaches for disease detection and diagnosis that benefit patients
2. LFIA are relatively inexpensive rapid tests that can be multiplexed with several test areas, developed using multicolored nanoparticles, and analyzed using imaging software and straightforward computational methods (principal component analysis) to yield clear test results.

Future Issues:

1. How will the diagnostics community incorporate rapid diagnostics data into medical records and shared public health resources? Currently, virus diagnostic results are generally not part of the HL7 interoperable medical record.

2. How can the culture of the diagnostics industry be changed from being reactive (generating diagnostics after an outbreak has occurred) to proactive (preparing reagents for pathogen diagnostics in advance of outbreaks)?

DISCLOSURE STATEMENT

Irene Bosch and Lee Gehrke are co-founders of E25Bio. James J. Collins is a co-founder and director of Sherlock Biosciences.

ACKNOWLEDGMENTS

We apologize to all investigators whose valuable research was not cited appropriately in this text because of limited space. We are grateful to our many collaborators around the world who have generously provided samples and thoughtful critiques during the course of this work.

References Cited

1. Banerjee R, Jaiswal A. 2018. Recent advances in nanoparticle-based lateral flow immunoassay as a point-of-care diagnostic tool for infectious agents and diseases. *Analyst* 143:1970-96
2. Wild D. 2013. The Immunoassay Handbook. In *Theory and applications of ligand binding, ELISA and related techniques*. The Boulevard, Langford Lane, Kidlington, Oxford, OX5 1GB, UK: Elsevier. Fourth ed.
3. Leuvering JH, Thal PJ, van der Waart M, Schuurs AH. 1980. Sol particle immunoassay (SPIA). *J. Immunoassay*. 1(1):77–91
4. Isaacs FJ, Dwyer DJ, Ding CM, Pervouchine DD, Cantor CR, Collins JJ. 2004. Engineered riboregulators enable post-transcriptional control of gene expression. *Nature Biotechnology* 22:841-7
5. Cameron DE, Bashor CJ, Collins JJ. 2014. A brief history of synthetic biology. *Nature Reviews Microbiology* 12:381-90
6. Elowitz MB, Leibler S. 2000. A synthetic oscillatory network of transcriptional regulators. *Nature* 403:335-8
7. Gardner TS, Cantor CR, Collins JJ. 2000. Construction of a genetic toggle switch in Escherichia coli. *Nature* 403:339-42
8. Slomovic S, Pardee K, Collins JJ. 2015. Synthetic biology devices for in vitro and in vivo diagnostics. *Proceedings of the National Academy of Sciences of the United States of America* 112:14429-35

9. Glushakova LG, Alto BW, Kim MS, Hutter D, Bradley A, et al. 2019. Multiplexed kit based on Luminex technology and achievements in synthetic biology discriminates Zika, chikungunya, and dengue viruses in mosquitoes. *Bmc Infectious Diseases* 19

10. McGregor AC, Moore DA. 2015. Infectious causes of fever of unknown origin. *Clinical Medicine* 15:285-7

11. Bosch I, de Puig H, Hiley M, Carre-Camps M, Perdomo-Celis F, et al. 2017. Rapid antigen tests for dengue virus serotypes and Zika virus in patient serum. *Science Translational Medicine* 9

12. de Puig H, Federici S, Baxamusa SH, Bergese P, Hamad-Schifferli K. 2011. Quantifying the Nanomachinery of the Nanoparticle-Biomolecule Interface. *Small* 7

13. de Puig H, Tam JO, Yen C-W, Gehrke L, Hamad-Schifferli K. 2015. The extinction coefficient of gold nanostars. *Journal of Physical Chemistry C* 119:17408–15

14. Tam JO, de Puig H, Yen C-w, Bosch I, Gómez-Márquez J, et al. 2016. A comparison of nanoparticle-antibody conjugation strategies in sandwich immunoassays. *Journal of Immunoassay and Immunochemistry*:1-23

15. Yen C-W, de Puig H, Tam JO, Gomez-Marquez J, Bosch I, et al. 2015. Multicolored silver nanoparticles for multiplexed disease diagnostics: distinguishing dengue, yellow fever, and Ebola viruses. *Lab on a chip* 15:1638-41

16. Homan KA, Souza M, Truby R, Luke GP, Green C, et al. 2012. Silver Nanoplate Contrast Agents for in Vivo Molecular Photoacoustic Imaging. *Acs Nano* 6:641-50

17. de Puig H, Bosch I, Gehrke L, Hamad-Schifferli K. 2017. Challenges of the Nano-Bio Interface in Lateral Flow and Dipstick Immunoassays. *Trends in Biotechnology* 35:1169-80

18. Mullis K, Faloona F, Scharf S, Saiki R, Horn G, Erlich H. 1992. Specific enzymatic amplification of DNA in vitro: the polymerase chain reaction. 1986. *Biotechnology (Reading, Mass.)* 24:17-27

19. Saiki RK, Scharf S, Faloona F, Mullis KB, Horn GT, et al. 1992. Enzymatic amplification of beta-globin genomic sequences and restriction site analysis for diagnosis of sickle cell anemia. 1985. *Biotechnology (Reading, Mass.)* 24:476-80

20. Zarei M. 2017. Advances in point-of-care technologies for molecular diagnostics. *Biosensors & Bioelectronics* 98:494-506

21. Loonen AJ, Schuurman R, van den Brule AJ. 2012. Highlights from the 7th European meeting on molecular diagnostics. *Expert review of molecular diagnostics* 12:17-9

22. Bar T, Kubista M, Tichopad A. 2012. Validation of kinetics similarity in qPCR. *Nucleic Acids Research* 40:1395-406

23. Roper MG, Easley CJ, Landers JP. 2005. Advances in polymerase chain reaction on microfluidic chips. *Analytical Chemistry* 77:3887-93

24. Mayboroda O, Katakis I, O'Sullivan CK. 2018. Multiplexed isothermal nucleic acid amplification. *Analytical Biochemistry* 545:20-30

25. Li J, Macdonald J. 2015. Advances in isothermal amplification: novel strategies inspired by biological processes. *Biosensors & Bioelectronics* 64:196-211

26. Giuffrida MC, Spoto G. 2017. Integration of isothermal amplification methods in microfluidic devices: Recent advances. *Biosensors & Bioelectronics* 90:174-86

27. Deiman B, van Aarle P, Sillekens P. 2002. Characteristics and applications of nucleic acid sequence-based amplification (NASBA). *Molecular Biotechnology* 20:163-79

28. Pardee K, Green AA, Ferrante T, Cameron DE, DaleyKeyser A, et al. 2014. Paper-Based Synthetic Gene Networks. *Cell* 159:940-54

29. Pardee K, Green AA, Takahashi MK, Braff D, Lambert G, et al. 2016. Rapid, Low-Cost Detection of Zika Virus Using Programmable Biomolecular Components. *Cell* 165:1255-66

30. Green AA, Silver PA, Collins JJ, Yin P. 2014. Toehold Switches: De-Novo-Designed Regulators of Gene Expression. *Cell* 159:925-39

31. Takahashi MK, Tan X, Dy AJ, Braff D, Akana RT, et al. 2018. A low-cost paper-based synthetic biology platform for analyzing gut microbiota and host biomarkers. *Nature Communications* 9

32. Gu W, Crawford ED, O'Donovan BD, Wilson MR, Chow ED, et al. 2016. Depletion of Abundant Sequences by Hybridization (DASH): using Cas9 to remove unwanted high-abundance species in sequencing libraries and molecular counting applications. *Genome Biology* 17

33. Muller V, Rajer F, Frykholm K, Nyberg LK, Quaderi S, et al. 2016. Direct identification of antibiotic resistance genes on single plasmid molecules using CRISPR/Cas9 in combination with optical DNA mapping. *Scientific Reports* 6

34. Zhang BB, Wang Q, Xu XH, Xia Q, Long FF, et al. 2018. Detection of target DNA with a novel Cas9/sgRNAs-associated reverse PCR (CARP) technique. *Analytical and Bioanalytical Chemistry* 410:2889-900

35. Lee SH, Yu J, Hwang GH, Kim S, Kim HS, et al. 2017. CUT-PCR: CRISPR-mediated, ultrasensitive detection of target DNA using PCR. *Oncogene* 36:6823-9

36. Zhang BB, Xia Q, Wang Q, Xia XY, Wang JK. 2018. Detecting and typing target DNA with a novel CRISPR-typing PCR (ctPCR) technique. *Analytical Biochemistry* 561:37-46

37. Wang Q, Zhang BB, Xu XH, Long FF, Wang JK. 2018. CRISPR-typing PCR (ctPCR), a new Cas9-based DNA detection method. *Scientific Reports* 8

38. Koo B, Kim DE, Kweon J, Jin CE, Kim SH, et al. 2018. CRISPR/dCas9-mediated biosensor for detection of tick-borne diseases. *Sensors and Actuators B-Chemical* 273:316-21

39. Hajian R, Balderston S, Tran T, deBoer T, Etienne J, et al. 2019. Detection of unamplified target genes via CRISPR–Cas9 immobilized on a graphene field-effect transistor. *Nature Biomedical Engineering* 3:427 – 37

40. Guk K, Keem JO, Hwang SG, Kim H, Kang T, et al. 2017. A facile, rapid and sensitive detection of MRSA using a CRISPR-mediated DNA FISH method, antibody-like dCas9/sgRNA complex. *Biosensors & Bioelectronics* 95:67-71

41. Gootenberg JS, Abudayyeh OO, Lee JW, Essletzbichler P, Dy AJ, et al. 2017. Nucleic acid detection with CRISPR-Cas13a/C2c2. *Science* 356:438-42

42. Gootenberg JS, Abudayyeh OO, Kellner MJ, Joung J, Collins JJ, Zhang F. 2018. Multiplexed and portable nucleic acid detection platform with Cas13, Cas12a, and Csm6. *Science* 360:439-44

43. Myhrvold C, Freije CA, Gootenberg JS, Abudayyeh OO, Metsky HC, et al. 2018. Field-deployable viral diagnostics using CRISPR-Cas13. *Science* 360:444-8

44. Chen JS, Ma EB, Harrington LB, Da Costa M, Tian XR, et al. 2018. CRISPR-Cas12a target binding unleashes indiscriminate single-stranded DNase activity. *Science* 360:436-9

45. Harrington LB, Burstein D, Chen JS, Paez-Espino D, Ma E, et al. 2018. Programmed DNA destruction by miniature CRISPR-Cas14 enzymes. *Science* 362:839-+

46. Bossuyt PMM, Reitsma JB, Linnet K, Moons KGM. 2012. Beyond Diagnostic Accuracy: The Clinical Utility of Diagnostic Tests. *Clinical Chemistry* 58:1636-43

47. De Paoli P. 2005. Biobanking in microbiology: From sample collection to epidemiology, diagnosis and research. *Fems Microbiology Reviews* 29:897-910

48. Dehnavieh R, Haghdoost A, Khosravi A, Hoseinabadi F, Rahimi H, et al. 2019. The District Health Information System (DHIS2): A literature review and meta-synthesis of its strengths and operational challenges based on the experiences of 11 countries. *Health Information Management Journal* 48:62-75

Figure Captions

Figure 1. Matrix for testing monoclonal antibodies in pairs to detect and distinguish dengue and Zika virus NS1 proteins. (Reprinted from (11) with permission).

Figure 2. Multiplexed detection of dengue, Zika, and chikungunya viruses. The vertical axis labels denote rows of immobilized antibodies. TD: anti-dengue NS1 protein; TZ; anti-Zika virus NS1 protein; TC: anti-Chikungunya envelope protein. The horizontal axis labels refer to the antigen(s) present in the samples that were run. D: dengue NS1 protein; Z: Zika virus NS1 protein; C: Chikungunya envelope protein; JEV: Japanese Encephalitis virus; TBEV: Tick-borne Encephalitis virus; WNV:West Nile virus ; YFV: Yellow Fever virus. ø: Negative, uninfected control.

Figure 3. Multicolored silver nanoparticles used to detect and distinguish among Yellow Fever virus, Ebola Virus, and Dengue Virus NS1 proteins. Reprinted from (15) with permission.

Figure 4: a) Toehold riboregulator for RNA detection. The toehold switch RNA sensor is designed with a toehold region (a+b) complementary to the target trigger RNA (a* + b*). In the OFF state, translation is inhibited by the sequestering of the RBS in a hairpin loop. When target trigger RNA is present, it binds the corresponding toehold region on the switch RNA, opening the hairpin enabling reporter gene translation. Active toehold switches are modular and can produce output proteins that produce fluorescence (GFP)

luminescence (Luc), or a color change visible to the naked eye (LacZ). b) Sequence information from online databases can be used to design toehold switch RNA sensors in silico. Sensors can be freeze-dried with transcription and translation cell-free extracts to be deployed in the field as diagnostics that can be stable for over one year at room temperature. Diagnostics can be activated upon rehydration. Color change visible to the naked eye can be observed through the expression of LacZ, where a color change from yellow to purple indicates that toehold switches were activated by the trigger. Adapted with permission from (28) and (29)

Figure 5: a) Schematic of toehold-Cas9 genotyping of single nucleotide polymorphisms (SNP) for Zika virus. A synthetic trigger sequence is attached to a NASBA-amplified RNA fragment through reverse transcription. Then, Cas9 cleaves dsDNA sequences that contain a PAM site, leading to the production of full-length or truncated trigger RNA. Full-length trigger RNA contains the trigger H sequence, which activates a toehold switch sensor (sensor H). B) A SNP between African (GenBank: KF268950) and American (GenBank: KU312312) Zika strains at site 7330 disrupts a PAM site, This allows for Cas9-mediated DNA cleavage only in the American strain, and no color change is observed from inactive toeholds. Adapted with permission from (29)

Figure 6: a) Schematic of SHERLOCK. Trigger dsDNA or RNA can be amplified by isothermal recombinase polymerase amplification (RPA) or reverse transcription RPA (RT-RPA), respectively. T7 polymerase is then used to produce trigger RNA for Cas13 reaction. Upon activation, Cas13a engages in collateral cleavage of labeled non-target

RNA leading to an increase in fluorescence. B) Cas13a can be freeze-dried on paper and used for sensitive and specific detection of low atto-molar concentrations of ZIKV. C) Schematic of multiplexed SHERLOCK capitalizes on differential collateral activities of Cas13a/b orthologs. PsmCas13b, LwaCas13a and LcaCas13b have preferential collateral activities on specific orthogonal dinucleotide bases. D) (A) Schematic of lateral-flow detection with SHERLOCK. A reporter ssRNA molecule contains both biotin and FAM moieties. In the presence of the trigger sequence (+), Cas13a cleaves the ssRNA reporter and nanoparticles (NP) coated with an anti-FAM (αFAM) antibody reach the anti-Fc band, leading to observable signal in both the streptavidin band (S) and anti-Fc band (αFc). In contrast, when the trigger sequence is not present (-), NP accumulate in the streptavidin band (S) and no signal is observed in the anti-Fc band. Adapted with permission from (41) and (42)

Figures

Figure 1:

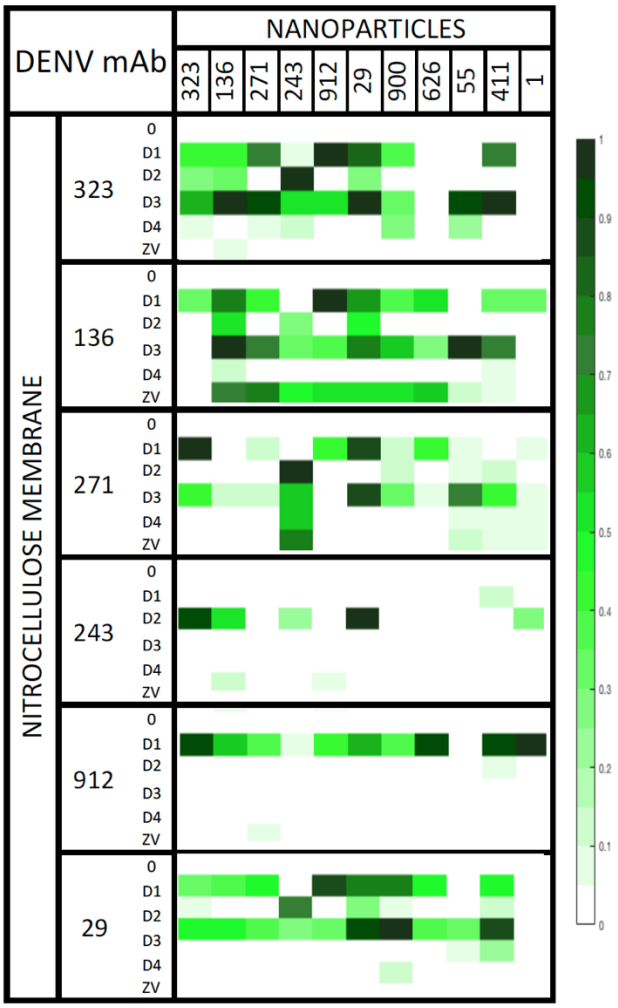

Figure 2:

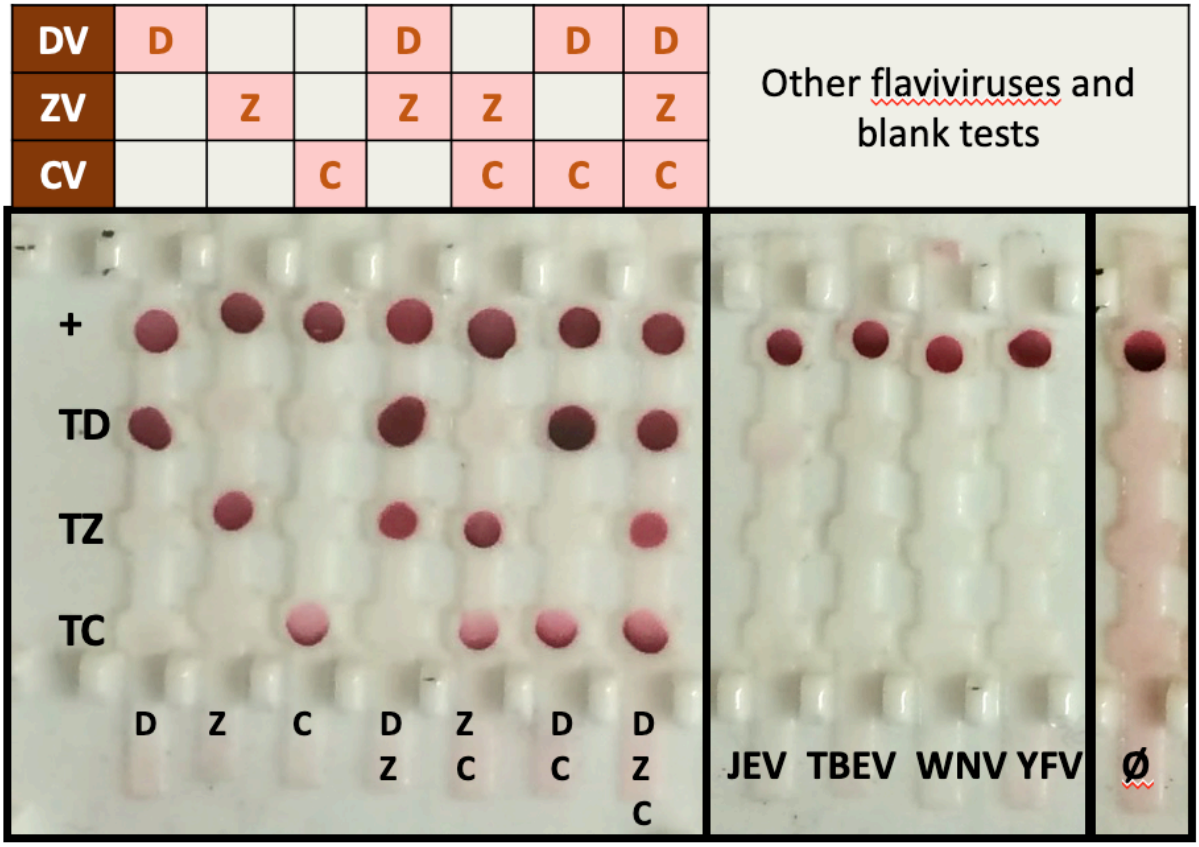
DV
ZV
CV
D
Z
C
D
Z
C
D
Z
C
D
Z
C
D
Z
C
D
Z
C
Other flaviviruses and blank tests
+
TD
TZ
TC
D
Z
C
D Z
Z C
D C
D Z C
JEV
TBEV
WNV
YFV
Ø

Figure 3:

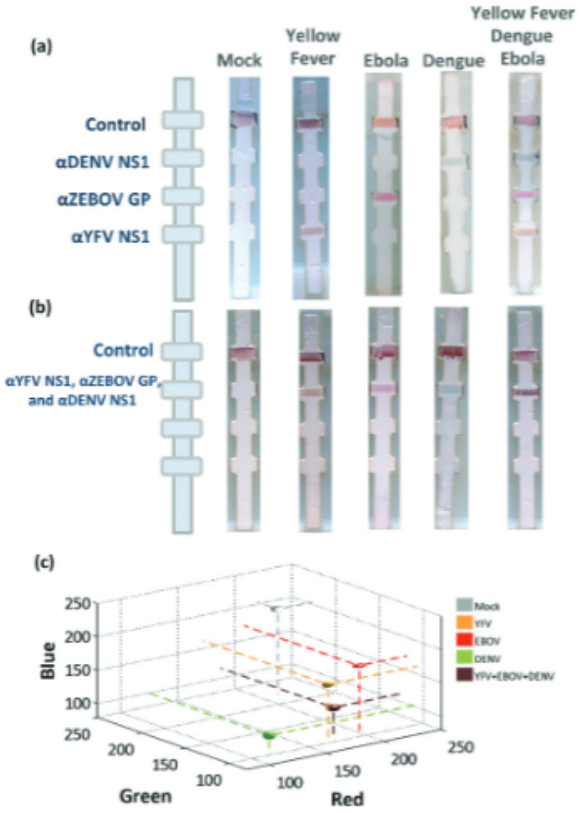
(a)
Mock
Yellow Fever
Ebola
Dengue
Yellow Fever Dengue Ebola
Control
αDENV NS1
αZEBOV GP
αYFV NS1
(b)
Control
αYFV NS1, αZEBOV GP, and αDENV NS1
(c)
Blue
Green
Red
250
200
150
100
Mock
YFV
EBOV
DENV
YFV+EBOV+DENV

Figure 4:

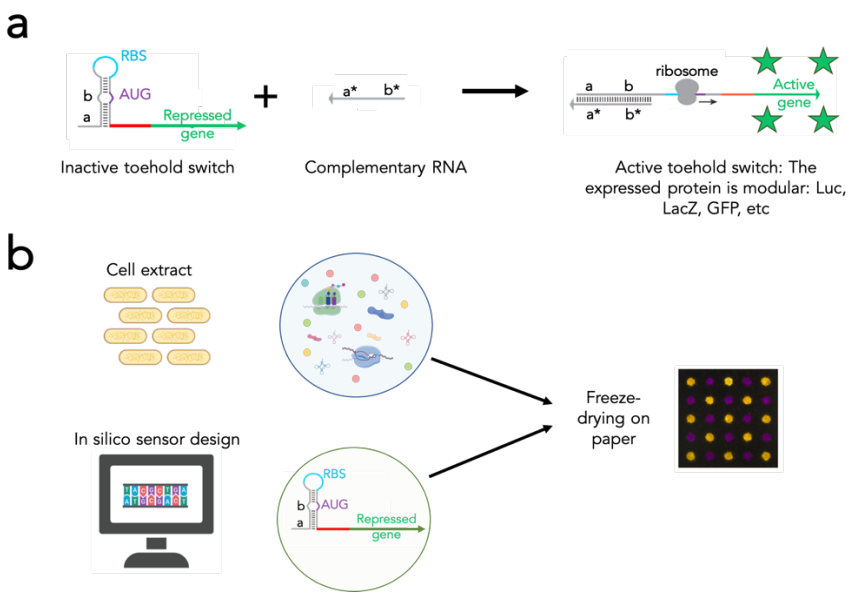
a
RBS
b
AUG
a
Repressed gene
a* b*
ribosome
a b
a* b*
Active gene
Inactive toehold switch
Complementary RNA
Active toehold switch: The expressed protein is modular: Luc, LacZ, GFP, etc
b
Cell extract
In silico sensor design
RBS
b
AUG
a
Repressed gene
Freeze-drying on paper

Figure 5:

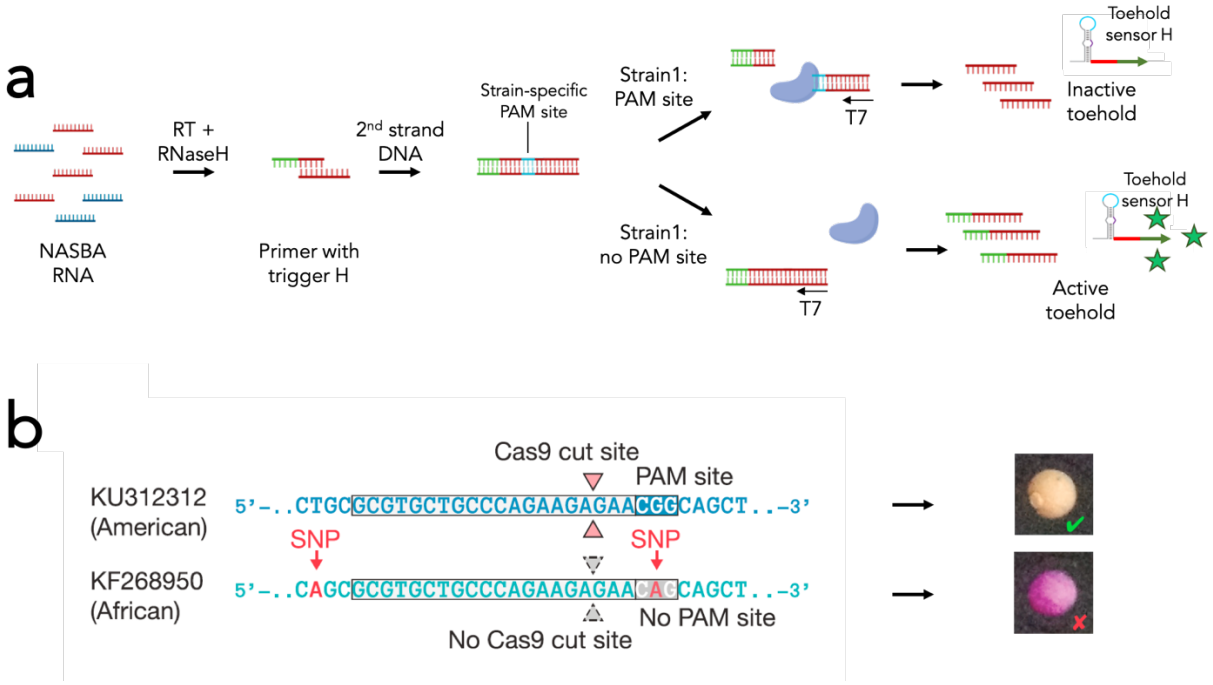
a
NASBA RNA
RT + RNaseH
Primer with trigger H
2nd strand DNA
Strain-specific PAM site
Strain1: PAM site
Strain1: no PAM site
T7
T7
Inactive toehold
Toehold sensor H
Active toehold
Toehold sensor H
b
Cas9 cut site
PAM site
KU312312 (American)
5'-..CTGCGCGTGCTGCCCAGAAGAGAACGGCAGCT..-3'
SNP
SNP
KF268950 (African)
5'-..CAGCGCGTGCTGCCCAGAAGAGAAAGCAGCT..-3'
No PAM site
No Cas9 cut site

Figure 6:

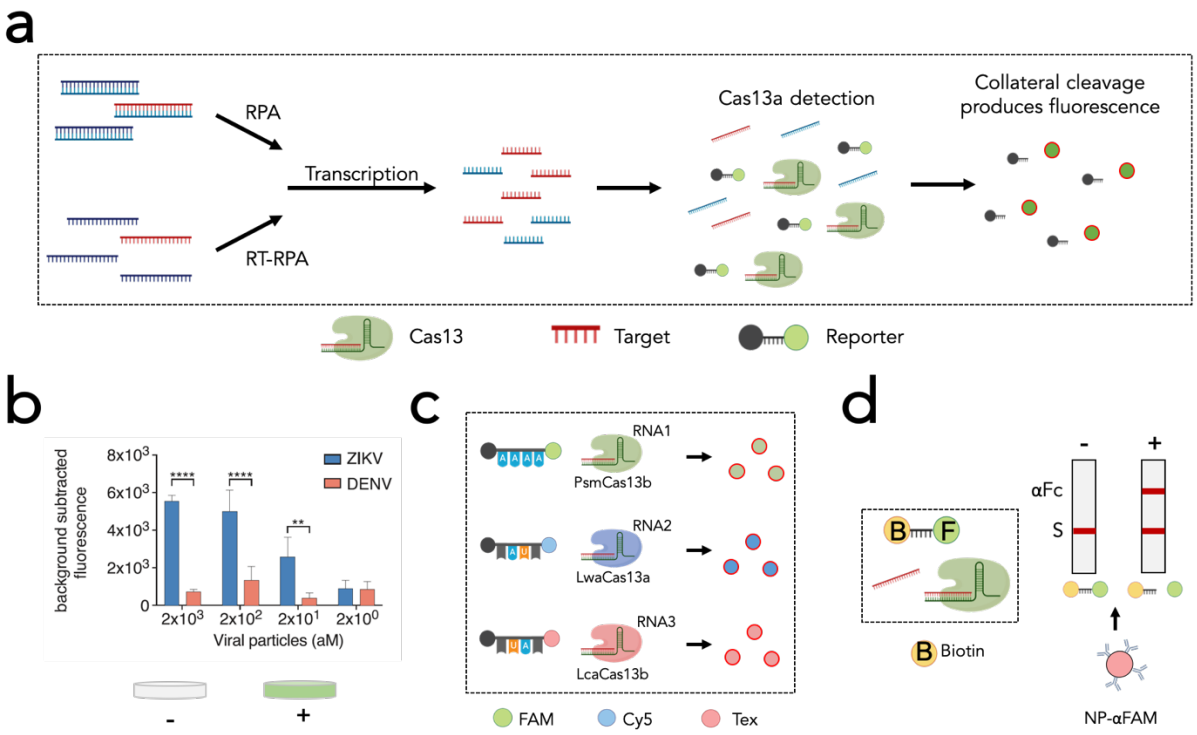
a
RPA
RT-RPA
Transcription
Cas13a detection
Collateral cleavage produces fluorescence
Cas13
Target
Reporter
b
background subtracted fluorescence
8x10^3
6x10^3
4x10^3
2x10^3
0
ZIKV
DENV
****
****
**
2x10^3
2x10^2
2x10^1
2x10^0
Viral particles (aM)
-
+
c
RNA1
PsmCas13b
RNA2
LwaCas13a
RNA3
LcaCas13b
FAM
Cy5
Tex
d
B
F
B Biotin
αFc
S
-
+
NP-αFAM